

NASA Contractor Report 195007

ICASE Report No. 94-94

IN-34

34452  
20P



# ICASE

## EFFECT OF CROSSFLOW ON GÖRTLER INSTABILITY IN INCOMPRESSIBLE BOUNDARY LAYERS

**Y. H. Zurigat**  
**M. R. Malik**

(NASA-CR-195007) EFFECT OF  
CROSSFLOW ON GOERTLER INSTABILITY  
IN INCOMPRESSIBLE BOUNDARY LAYERS  
Final Report (ICASE) 20 p

N95-18193

Unclas

G3/34 0034452

Contract NAS1-19480  
November 1994

Institute for Computer Applications in Science and Engineering  
NASA Langley Research Center  
Hampton, VA 23681-0001



Operated by Universities Space Research Association



# EFFECT OF CROSSFLOW ON GORTLER INSTABILITY IN INCOMPRESSIBLE BOUNDARY LAYERS

Y. H. Zurigat<sup>1</sup>  
Mechanical Engineering Department  
University of Jordan, Amman, Jordan

M. R. Malik<sup>2</sup>  
High Technology Corporation  
P.O. Box 7262, Hampton, VA 23666

## ABSTRACT

Linear stability theory is used to study the effect of crossflow on Görtler instability in incompressible boundary layers. The results cover a wide range of sweep angle, pressure gradient, and wall curvature parameters. It is shown that the crossflow stabilizes Görtler disturbances by reducing the maximum growth rate and shrinking the unstable band of spanwise wave numbers. On the other hand, the effect of concave wall curvature on crossflow instability is destabilizing. Calculations show that the changeover from Görtler to crossflow instabilities is a function of Görtler number, pressure gradient and sweep angle. The results demonstrate that Görtler instability may still be relevant in the transition process on swept wings even at large angles of sweep if the pressure gradient is sufficiently small. The influence of pressure gradient and sweep can be combined by defining a crossflow Reynolds number. Thus, the changeover from Görtler to crossflow instability takes place at some critical crossflow Reynolds number whose value increases with Görtler number.

---

<sup>1</sup>This research was supported by the National Aeronautics and Space Administration under NASA Contract No. NAS1-19480 while the author was in residence at the Institute for Computer Applications in Science and Engineering (ICASE), NASA Langley Research Center, Hampton, VA 23681.

<sup>2</sup> This research was supported by NASA Langley Research Center under Contract NAS1-19299.



## 1. Introduction

A problem of great practical interest in aerospace applications is the drag reduction on aircraft wings, nacelles, etc. This has stimulated a number of research efforts on laminar-turbulent transition phenomenon for effective application of laminar flow control (LFC) which offers significant potential for reducing drag on aerodynamic surfaces. The supercritical wing is an example of advanced designs of laminar-flow airfoils. This wing has two concave regions on its lower surface and, therefore, when it is swept, the flow is subject to not only crossflow instability but also possibly the Görtler instability. The crossflow instability is observed on swept wings and leads to streamwise corotating vortices while Görtler instability is identified by the formation of pairs of counterrotating vortices with their axes aligned with the flow direction.

In this paper, the effect of crossflow on Görtler instability is investigated. In the case of swept supercritical wing which supports both Görtler and crossflow instabilities a question arises as to which of these two vortex instabilities is significant for a given set of conditions. This question is also relevant for hypersonic flow ahead of engine inlet where concave curvature and some three-dimensionality are present either by design or inadvertently. Previous works addressing this problem are few and limited in scope and include theoretical works of Hall (1985), Collier and Malik (1987), Bassom and Hall (1991), and Blackaby and Choudhari (1993) and the experimental work of Kohama (1987) and more recently by Bippes (1994).

Hall (1985) studied the effect of crossflow on Görtler vortices for flow over an infinitely long swept cylinder using asymptotic analysis. He concluded that the crossflow has a stabilizing effect on Görtler vortices and that for large angles of sweep the Görtler instability does not exist. For the concave region of a supercritical wing, Collier and Malik (1987) used Orr-Sommerfeld approach and showed that at low sweep angles the instability is of Görtler type and as the sweep angle increases the instability becomes of crossflow type. They also showed that concave surface curvature has a destabilizing influence on crossflow instability. Using hot-wire anemometry and smoke-wire flow visualization techniques, Kohama (1987) observed Görtler instability in the concave region in the absence of sweep and crossflow instability for  $47^\circ$  of sweep. The relation between Görtler and crossflow vortices was further studied by Bassom and Hall (1991). They found that Görtler vortices cannot exist on swept wings when the angle of sweep exceeds  $20^\circ$ . Blackaby and Choudhari (1993) studied inviscid instability of three-dimensional boundary layers over both concave and convex surfaces. They also investigated the relation of this problem to the stability of stratified shear flows.

Most of the aforementioned theoretical studies were based on asymptotic analyses in the large Görtler number limit and within the framework of inviscid linear theory. Moreover, they were restricted to a single value of the pressure-gradient parameter ( $\beta_h = 0.5$ ). In this paper, we present detailed results on the effect of crossflow on Görtler vortex instability by using viscous analysis. The governing mean flow equations and linear stability analysis are presented in the next section followed by the results in section 3.

## 2. Problem Formulation

We consider a three-dimensional boundary-layer flow over a concave surface whose constant radius of curvature  $r^\dagger = 1/\kappa^\dagger$ . The streamwise, wall-normal and the spanwise coordinates are denoted as  $x = X/\ell_0$ ,  $y = Y/\ell_0$  and  $z = Z/\ell_0$ , respectively ( $y = 0$  denotes the wall), where the length scale  $\ell_0$  will be prescribed later. Let the  $x, y$  and  $z$  components of the velocity and pressure be given by

$$(u^\dagger, v^\dagger, w^\dagger) = U_e \{U(x, y) + u(x, y, z, t), V(x, y) + v(x, y, z, t), W + w(x, y, z, t)\} \quad (1)$$

$$p^\dagger = \rho U_e^2 (P + p(x, y, z, t)) \quad (2)$$

where the superscript  $\dagger$  represents a dimensional quantity and  $U_e$  is the velocity scale. Here  $U, V$  and  $W$  are mean-flow components whereas  $u, v, w$  represent the perturbation velocity components in  $x, y, z$  directions, respectively. Similarly,  $P$  and  $p$  represent the mean and perturbation pressures.

The mean flow investigated in this study is the Falkner-Skan-Cooke (FSC) boundary layer. We consider the chordwise potential flow velocity distribution:

$$U_\infty = cX^m$$

where the exponent  $m$  is related to the Hartree pressure gradient parameter  $\beta_h = 2m/(m+1)$  which defines the wedge half angle  $(\pi/2)\beta_h$ . The spanwise potential flow velocity component,  $W_\infty$ , parallel to the leading edge is constant. With the similarity variable  $\eta$  defined by  $\eta = Y/\ell$  where  $\ell = (\nu X/U_\infty)^{1/2}$ ,  $\nu$  the kinematic viscosity,  $U = \frac{U_\infty}{U_e} f'$ ,  $W = \frac{W_\infty}{U_e} g$ , the self-similar three-dimensional boundary layer equations are given by:

$$f''' + \frac{m+1}{2} ff'' + m(1-f'^2) = 0 \quad (3)$$

$$g'' + \frac{m+1}{2}fg' = 0 \quad (4)$$

where the primes denote differentiation with respect to  $\eta$ .

We assume that the Reynolds number is large and that the radius of curvature is much larger than the boundary-layer thickness,  $\delta$  (i.e.,  $k^\dagger\delta \ll 1$ ). In this case, if  $\kappa = \kappa^\dagger\ell_0$ , the equations governing the perturbation quantities are

$$\frac{\partial u}{\partial t} + U \frac{\partial u}{\partial x} + u \frac{\partial U}{\partial x} + V \frac{\partial u}{\partial y} + v \frac{\partial U}{\partial y} + W \frac{\partial u}{\partial z} + \kappa(Uv + Vu) + \frac{\partial p}{\partial x} - \frac{1}{R} \nabla^2 u = 0 \quad (5)$$

$$\frac{\partial v}{\partial t} + U \frac{\partial v}{\partial x} + u \frac{\partial V}{\partial x} + V \frac{\partial v}{\partial y} + v \frac{\partial V}{\partial y} + W \frac{\partial v}{\partial z} - 2\kappa Uu + \frac{\partial p}{\partial y} - \frac{1}{R} \nabla^2 v = 0 \quad (6)$$

$$\frac{\partial w}{\partial t} + U \frac{\partial w}{\partial x} + V \frac{\partial w}{\partial y} + W \frac{\partial w}{\partial z} + \frac{\partial p}{\partial z} - \frac{1}{R} \nabla^2 w = 0 \quad (7)$$

$$\frac{\partial u}{\partial x} + \frac{\partial v}{\partial y} + \frac{\partial w}{\partial z} + \kappa v = 0 \quad (8)$$

where

$$\nabla^2 = \frac{\partial^2}{\partial x^2} + \frac{\partial^2}{\partial y^2} + \frac{\partial^2}{\partial z^2} + \kappa \frac{\partial}{\partial y}.$$

The boundary conditions are

$$u = v = w = 0 \quad \text{at} \quad y = 0 \quad \text{and} \quad u \rightarrow 0, \quad v \rightarrow 0, \quad w \rightarrow 0, \quad \text{as} \quad y \rightarrow \infty \quad (9)$$

Here,  $\ell_0$  and  $U_e$  are constants so as to define Reynolds number  $R$  as

$$R = \frac{U_e \ell_0}{\nu}$$

where the length scale  $\ell_0 = \sqrt{\nu X_0 / U_e}$ ,  $X_0$  being the location (dimensional) of a reference streamwise station. In flows where Görtler vortex phenomenon constitutes the dominant primary instability, Görtler number is generally of  $O(20)$  where  $G$  is defined as

$$G = R \sqrt{\ell_0 \kappa^\dagger} \quad (10)$$

In the present paper, we solve the viscous linear stability equations under the parallel-flow approximation. While such an approximation is questionable for Görtler vortices at  $O(1)$  Görtler and wave numbers, it is less so for high Görtler numbers. The quasi-parallel approach, despite its limitations, provides a useful tool to study the link between Görtler and crossflow disturbances, including the effect of viscosity. Parabolized stability equations (Bertolotti et al. 1992, Malik and Li 1993) represent a more appropriate model for this problem, but the local approach adopted here allows parametric studies to be performed more efficiently. Except for flat walls ( $G = 0$ ) where only crossflow instability is relevant and for which quasi-parallel assumption has been commonly used, we will consider large Görtler numbers ( $G \geq 15$ ) so that the error introduced by the above approximation is minimized. For large Görtler numbers, the present results are at least as valid as the previous asymptotic results with the added effect of viscosity.

Under the parallel flow approximation ( $U = U(y)$ ,  $V = 0$ ,  $W = W(y)$ ) allows stationary disturbances of the form

$$\phi(x, y, z) = \hat{\phi}(y)e^{i(\alpha x + \beta z)} + c.c. \quad (11)$$

where  $\phi = [u, v, w, p]^T$  and *c.c.* stands for complex conjugate. Substituting Eq. (11) into Eqs. (5)–(8) yields the following ordinary differential equations

$$\xi \hat{u} + \left( \frac{dU}{dy} + \kappa U \right) \hat{v} + i\alpha \hat{p} = 0 \quad (12)$$

$$-2\kappa U \hat{u} + \xi \hat{v} + \frac{d\hat{p}}{dy} = 0 \quad (13)$$

$$\xi \hat{w} + i\beta \hat{p} = 0 \quad (14)$$

$$i\alpha \hat{u} + \frac{\partial \hat{v}}{\partial y} + i\beta \hat{w} + \kappa \hat{v} = 0 \quad (15)$$

where

$$\xi = i\alpha U + i\beta W - \frac{1}{R} \left[ -\alpha^2 - \beta^2 + \frac{d^2}{dy^2} + \kappa \frac{d}{dy} \right]$$

The boundary conditions for the above equations are

$$\hat{u}(0) = \hat{v}(0) = \hat{w}(0) = 0 \quad (16)$$



$$\hat{u} \rightarrow 0, \quad \hat{v} \rightarrow 0, \quad \hat{w} \rightarrow 0 \quad \text{as} \quad y \rightarrow \infty \quad (17)$$

Equations (12)–(15) along with homogeneous boundary conditions (16)–(17) constitute an eigenvalue problem

$$\alpha = \alpha(\beta) \quad (18)$$

which is solved by fourth-order accurate compact difference scheme described by Malik et al. (1982). As noted in Malik and Li (1993) and Masad and Malik (1994), the dominant curvature term for three-dimensional boundary-layer stability is the  $2\kappa U\hat{u}$  term in the normal momentum equation. An order of magnitude analysis of the Görtler vortex problem in two-dimensional flows leads to the same conclusion (Hall 1983).

### 3. Results

The results presented in this paper are obtained by solving the linear stability equations (12–17) for a Reynolds number of  $R = U_e \ell_0 / \nu = 1000$ . While the Görtler instability depends only on the value of the Görtler number (Eq. (10)), crossflow instability depends also on the value of Reynolds number, but at this high value of Reynolds number the dependence is weak since crossflow instability is basically inviscid in nature. Figure 1 (for  $\beta_h = 0.5$ ) shows the effect of sweep angle  $\Lambda$  in radians  $\Lambda = \tan^{-1}(W_\infty / U_\infty)$ , on spatial growth rate (scaled with  $\ell_0$ ) of stationary disturbances for different Görtler numbers. The corresponding streamwise wave numbers are shown in Fig. 2. In the absence of wall curvature (Fig. 1a) where the instability is of crossflow type the growth rate increases with the increase in the sweep angle. As Görtler number increases (Figs. 1b, c, d) two distinct features of the growth rate are observed; at low sweep angles the instability is of Görtler type and as the sweep angle increases beyond a certain limit the instability becomes of crossflow type. This sweep angle limit corresponding to the changeover from Görtler to crossflow instabilities is dependent on Görtler number and as will be seen below, on the pressure-gradient parameter  $\beta_h$ . As shown in Fig. 1 the "changeover" sweep angle increases with the increase in Görtler number. For  $G = 50$ , the changeover occurs at approximately  $\Lambda = 0.4$  radians ( $23^\circ$ ). The corresponding value reported by Bassom and Hall (1991) for the large Görtler number inviscid limit is  $\Lambda = 20^\circ$ . Thus our viscous calculation using  $\beta_h = 0.5$ ,  $G = 50$  yields a result close to that obtained by the inviscid theory.

In the sweep angle range over which Görtler instability is present, we notice (see Figs. 1 b,c,d) that the maximum growth rate decreases with the increase in the sweep angle. Moreover, the

unstable band of spanwise wave numbers shrinks with the increase in crossflow; thus, the effect of crossflow on Görtler disturbance is a stabilizing one. It is also to be noted that in the inviscid Görtler problem, only the left branch of the growth curve is present. The right branch which gives rise to a neutral point at high wave numbers is due to the effect of viscosity. This right neutral point moves to lower wave numbers when sweep angle increases as noted above.

Another observation is made here with regards to the influence of wall curvature on crossflow instability. The results shown in Fig. 1 are replotted in Fig. 3 for six different sweep angles. It is seen that concave wall curvature enhances crossflow instability (see Figs. 3 c,d,e,f), as was earlier shown by Collier and Malik (1987). In contrast, convex wall curvature stabilizes crossflow disturbances (Malik and Balakumar 1993, Masad and Malik 1994). These effects are also consistent with the inviscid results of Blackaby and Choudhari (1993).

An important parameter relevant in three-dimensional boundary-layer flows is the crossflow Reynolds number defined as

$$R_{cf} = \bar{U}_c \delta_{0.1} / \nu \quad (19)$$

where  $\bar{U}_c$  is the magnitude of the maximum crossflow velocity (in a direction which is at right angle to the local inviscid streamline) within the boundary layer and  $\delta_{0.1}$  is the boundary-layer thickness within which the crossflow velocity drops to 10 percent of  $\bar{U}_c$ .

In Fig. 4, the variation of crossflow Reynolds number with sweep angle is plotted for different  $\beta_h$ . It is clear that the crossflow Reynolds number increases pressure gradient for any sweep angle. Therefore, the crossflow instability is expected to be enhanced with pressure gradient. The results in Figs. 1–3 were obtained for a single value of the pressure gradient ( $\beta_h = 0.5$ ). The results for different values of pressure gradient parameter are presented in Fig. 5. The effect of pressure gradient is seen to influence Görtler and crossflow instabilities in two different ways. As the pressure gradient becomes more favorable, the maximum Görtler vortex growth rate decreases and the unstable band of spanwise wave numbers shrinks. In contrast, the crossflow instability increases with the pressure gradient. Thus, the increase in  $\beta_h$  destabilizes crossflow vortices and stabilizes Görtler vortex instability. This is a direct result of increase in the crossflow velocity (and consequently  $R_{cf}$ ) with pressure gradient.

For any given sweep angle, results such as those in Fig. 5 enable us to identify the pressure gradient at which Görtler instability is destroyed in favor of crossflow instability. Alternatively, for any given pressure gradient the sweep angle corresponding to the changeover from Görtler to

crossflow instabilities can be determined. When the maximum growth rate is calculated for different values of pressure gradient and sweep angles and the results are plotted in the manner shown in Fig. 6, the following observations can be made:

- (1) Each curve corresponding to a given sweep angle has, when applicable, two branches of opposite slopes. The lower branch (negative slope) corresponds to Görtler instability while the upper branch corresponds to crossflow instability.
- (2) For small sweep angles ( $\Lambda \approx 0.1$  radians) the instability is of Görtler type for any pressure gradient parameter  $\beta_h$ .
- (3) For large sweep angles Görtler instability is restricted to small pressure gradients.

Thus, a reduction in the pressure gradient renders instability of the Görtler type. For example, for  $G = 15$  (Fig. 6a) Görtler instability is the dominant mechanism for pressure gradients  $\beta_h < 0.25$  and sweep angles greater than 0.3 whereas for  $G = 30$  (Fig. 6b) this occurs at higher pressure gradients. Thus, Görtler instability may be the cause of transition in incompressible flow even at high angles of sweep if the pressure gradient is sufficiently small but nonzero. For zero-pressure gradient,  $R_{cf} = 0$  for any sweep angle and there is no crossflow instability.

In three-dimensional boundary-layer transition, crossflow Reynolds number,  $R_{cf}$ , is used as a governing parameter in correlating the transition onset. In this study we look into a possible correlation for the changeover from Görtler to crossflow instability in terms of  $R_{cf}$ . Figure 7 shows the variation of maximum growth rate with  $R_{cf}$  for different pressure gradient levels while Fig. 8 shows the results for fixed sweep angles. The  $R_{cf}$  double values (e.g., Fig. 7b for  $\beta_h = 0.5$ ) are a result of the  $R_{cf}$  variation with sweep angle shown in Fig. 4 as  $\Lambda$  increases beyond a value of 0.76 radians. In Figs. 7a,b for any fixed pressure gradient, the minimum value of the maximum growth rate, when applicable, corresponds to the changeover from Görtler (left branch) to crossflow (right branch) instability. The corresponding  $R_{cf}$  denoted as  $R_{cfc}$  (the changeover  $R_{cf}$ ) is seen to be a function of pressure gradient, sweep and the Görtler number. However, the strong dependence of  $R_{cfc}$  is on Görtler number. A comparison of Figs. 7(a) and 8(a) for  $G = 15$  shows that  $R_{cfc} \sim 70-100$  while a similar comparison of Figs. 7(b) and 8(b) for  $G = 30$  shows that the changeover takes place at  $R_{cfc} \sim 150-200$ . Thus  $R_{cf}$  is an important parameter for determining the changeover from Görtler to crossflow instability but its value increases with Görtler number.

The above results represent an important guide for the design of advanced LFC wings. However, it is cautioned that they are based upon local theory. Clearly, whether crossflow can destroy Görtler vortices depends upon nonlinear effects and the strength of the vortex which is related to the upstream history (distribution of wall curvature and pressure gradient for a given leading-edge sweep) and this evolution is best described by nonlinear parabolized stability equations.

#### **4. Conclusions**

An investigation of the relation between Görtler and crossflow instabilities of incompressible, three-dimensional boundary-layer flow is carried out using linear stability theory. The results cover a wide range of sweep angles, pressure gradients and wall curvature. It is shown that Görtler instability may persist even at large sweep angles when the pressure gradient is small. The results demonstrate the stabilizing effect of crossflow on Görtler disturbances and the destabilizing effect of concave wall curvature on crossflow disturbances. It is shown that the changeover from Görtler to crossflow instabilities is governed by crossflow Reynolds number. The value of crossflow Reynolds number at which the instabilities are switched increases with increasing Görtler number.

## REFERENCES

- Bassom, A. P. and Hall, P., Vortex instabilities in three-dimensional boundary layers: the relationship between Görtler and crossflow vortices, *J. Fluid Mech.* **232**, 647, 1991.
- Bertolotti, F. P., Herbert, Th. and Spalart, P. R., Linear and nonlinear stability of the Blasius boundary layer, *J. Fluid Mech.* **242**, 441, 1992.
- Bippes, H. Instability developing in the three-dimensional boundary layer on concave and convex curved surface, IUTAM Symposium on Laminar-Turbulent Transition, Sendai, Japan., Sept. 5-9, 1994.
- Blackaby, N. D. and Choudhari, M., Inviscid vortex motions in weakly three-dimensional boundary layers and their relation with instabilities in stratified shear flows, *Proc. R. Soc. Lond.* **A440**, 701, 1993.
- Collier, F. S., Jr. and Malik, M. R., Stationary disturbances in three-dimensional boundary layers over concave surfaces, *AIAA Paper* 87-1412, 1987.
- Hall, P., The linear development of Gortler vortices in growing boundary layer, *J. Fluid Mech.* **30**, 41, 1983.
- Hall, P., The Görtler vortex instability mechanism in three-dimensional boundary layers, *Proc. R. Soc. Lond.* **A399**, 135, 1985.
- Kohama, Y., Three-dimensional boundary layer transition on a concave-convex curved wall, *Proc. IUTAM Symposium on Turbulence Management and Relaminarization*, eds., R. Narasimha and H. Liepmann, Bangalore, India, Springer-Verlag, p. 215, 1987.
- Malik, M. R. and Li, F. Secondary instability of Görtler and crossflow vortices, in *Proc. Internal Symp. on Aerospace & Fluid Science*, Institute of Fluid Science, Tohoku University, Sendai, Japan, p. 460, 1993.
- Malik, M. R., Chuang, S., and Hussaini, M. Y., Accurate numerical solution of compressible stability equations, *ZAMP* **33**, 189, 1982.
- Malik, M. R. and Balakumar, P., Linear stability of three-dimensional boundary layers: effects of curvature and non-parallelism, *AIAA Paper* 93-0079, 1993.
- Masad, J. A. and Malik, M. R., Effects of body curvature and nonparallelism on the stability of flow over a swept cylinder, *Phys. Fluids* **6(7)**, 2363, 1994.

## Figure Captions

Figure 1. Effect of sweep angle  $\Lambda$  (radians) on spatial growth rate of stationary disturbances in Falkner-Skan-Cooke (FSC) boundary layer for different values of Görtler numbers.

Figure 2. Variation of streamwise wave number with spanwise wave number for different sweep angles and Görtler numbers.

Figure 3. Effect of wall curvature on spatial growth rate of Görtler and crossflow disturbances in FSC boundary layer for different values of sweep angle  $\Lambda$ .

Figure 4. Variation of crossflow Reynolds number with pressure gradient and sweep.

Figure 5. Effect of pressure gradient on spatial growth rate of stationary crossflow and Görtler disturbances of FSC boundary layers.

Figure 6. Effect of sweep angle and pressure gradient on maximum growth rate of stationary crossflow and Görtler disturbances of FSC boundary layer for two different Görtler numbers.

Figure 7. Variation of maximum growth rate with  $R_{cf}$  for fixed  $\beta_h$ .

Figure 8. Variation of maximum growth rate with  $R_{cf}$  for fixed  $\Lambda$ .

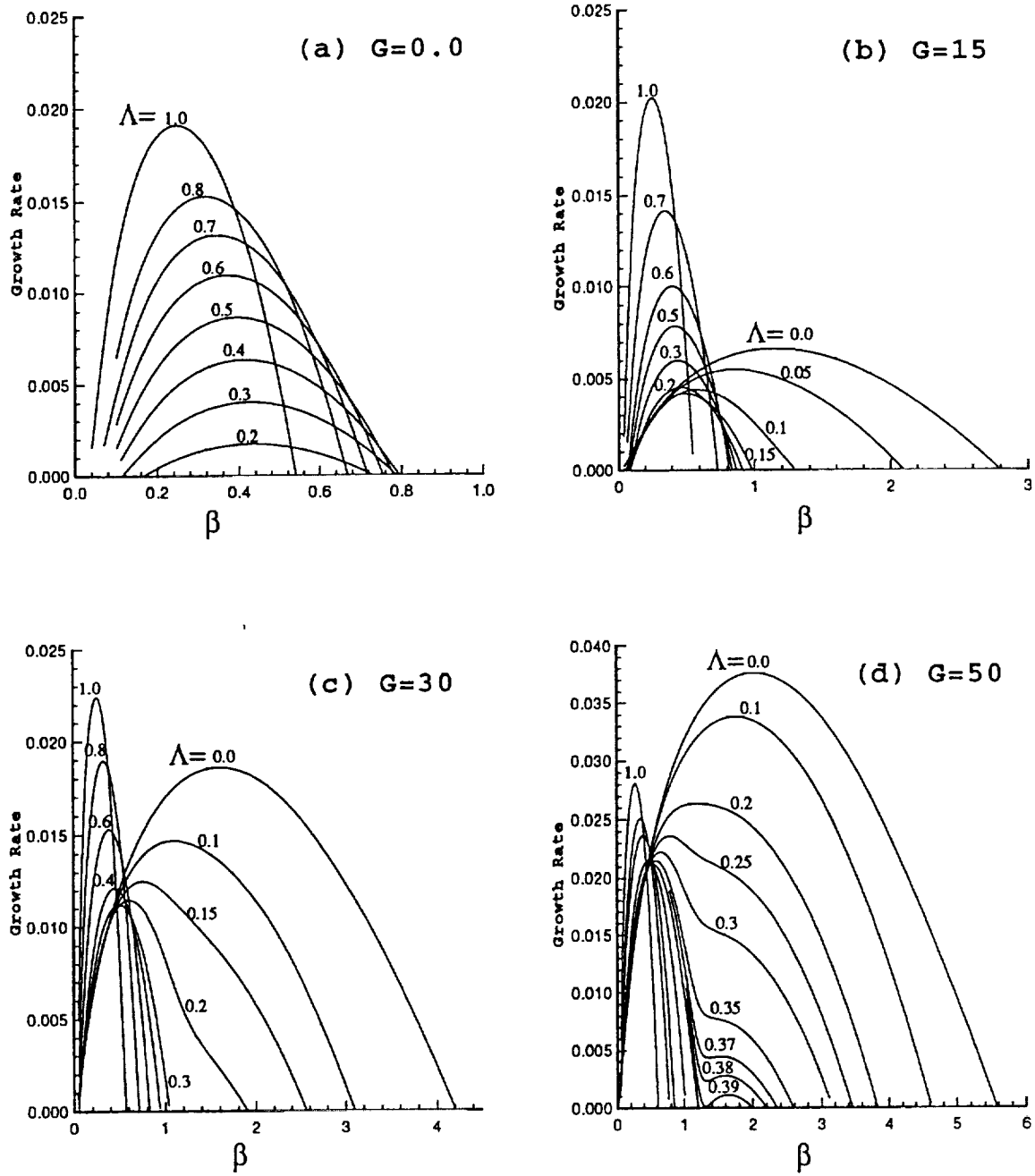


Figure 1. Effect of sweep angle  $\Lambda$  (radians) on spatial growth rate of stationary disturbances in Falkner-Skan-Cooke (FSC) boundary layer for different values of Görtler numbers.

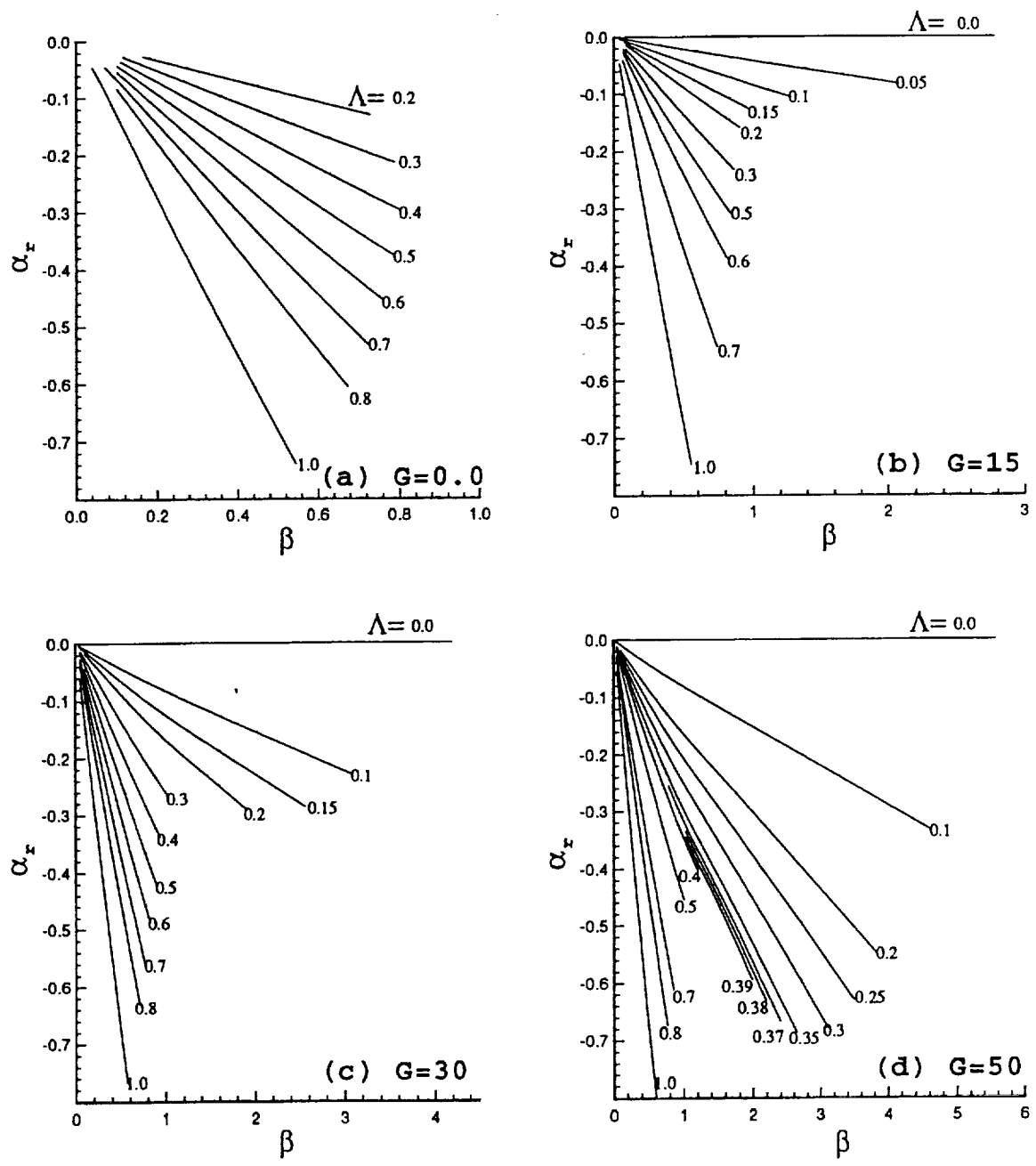


Figure 2. Variation of streamwise wave number with spanwise wave number for different sweep angles and Görtler numbers.



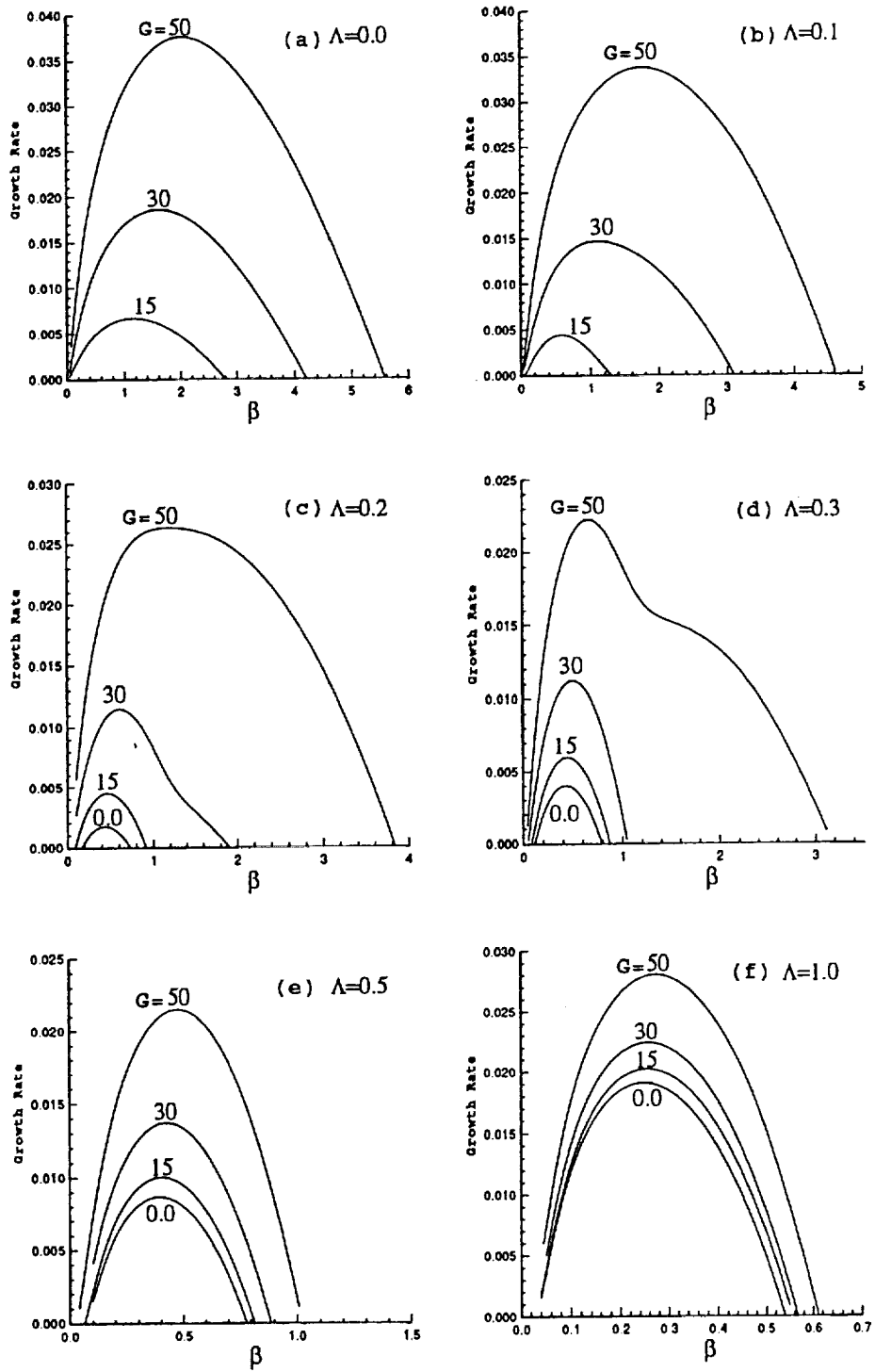


Figure 3. Effect of wall curvature on spatial growth rate of Görtler and crossflow disturbances in FSC boundary layer for different values of sweep angle  $\Lambda$ .

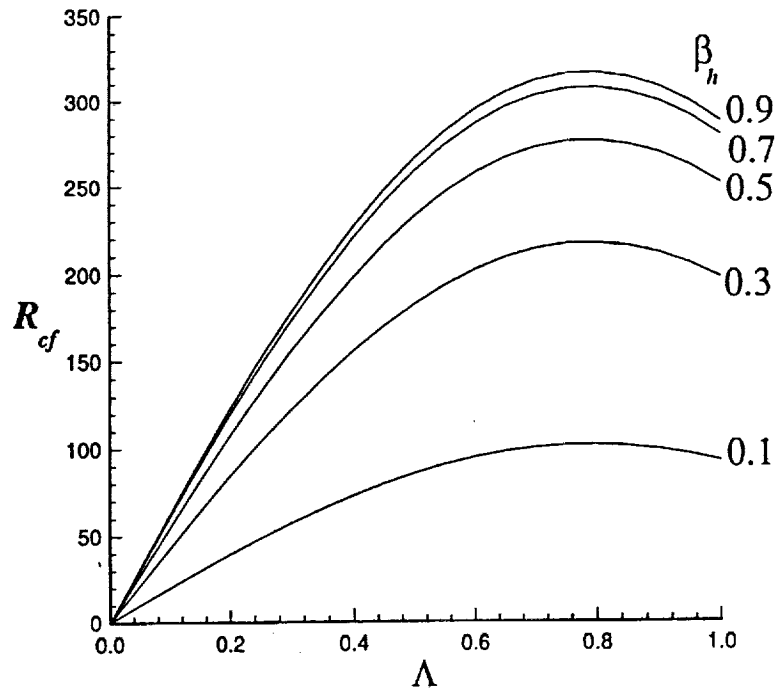


Figure 4. Variation of crossflow Reynolds number with pressure gradient and sweep.

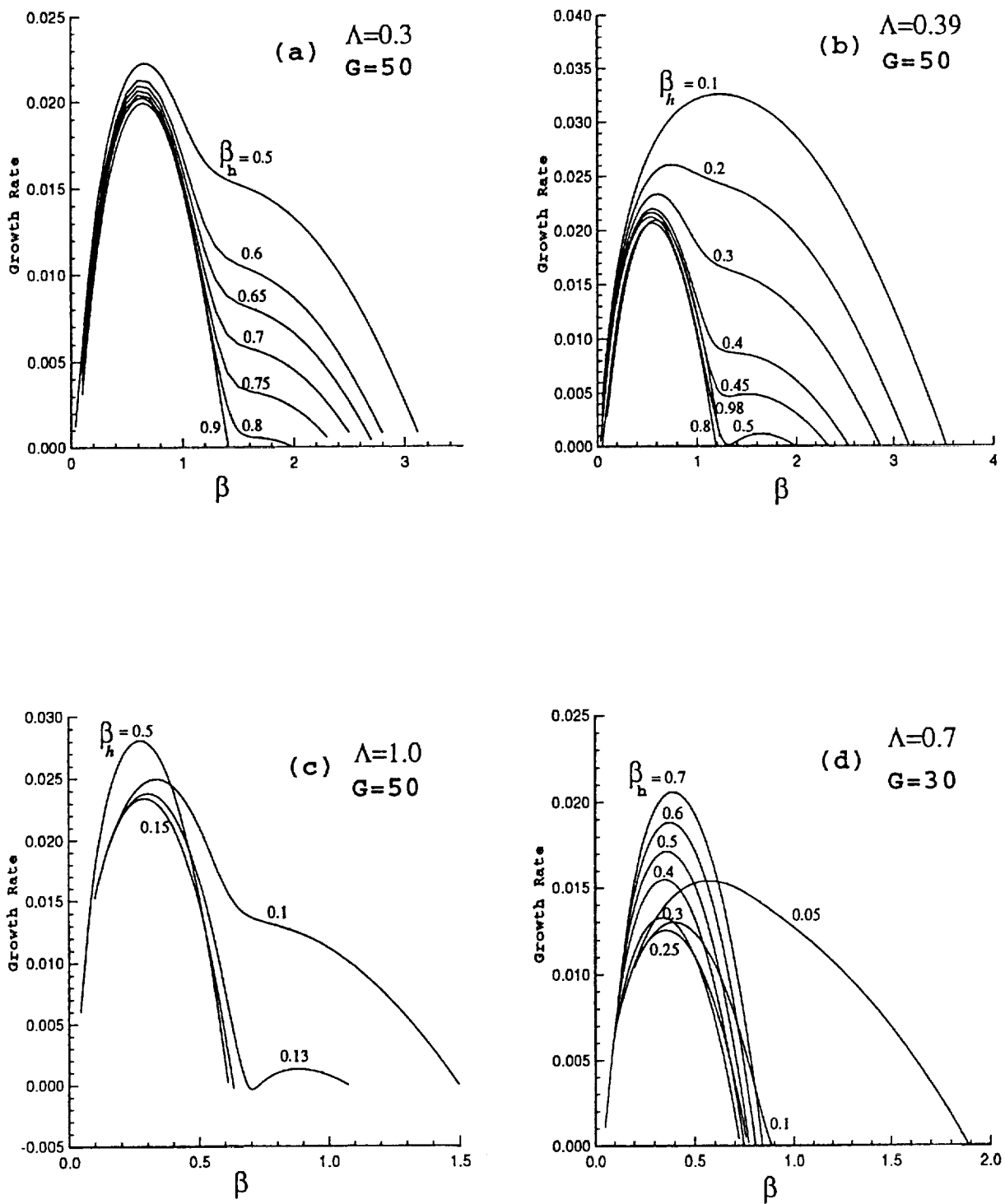


Figure 5. Effect of pressure gradient on spatial growth rate of stationary crossflow and Görtler disturbances of FSC boundary layers.

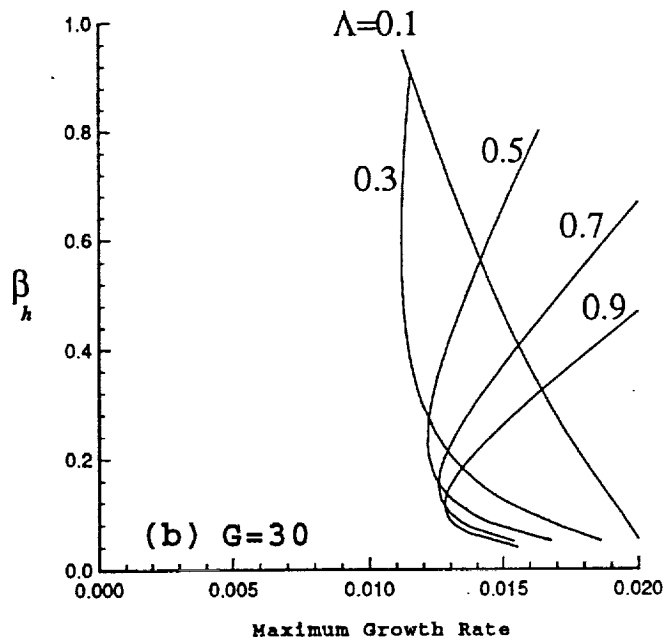
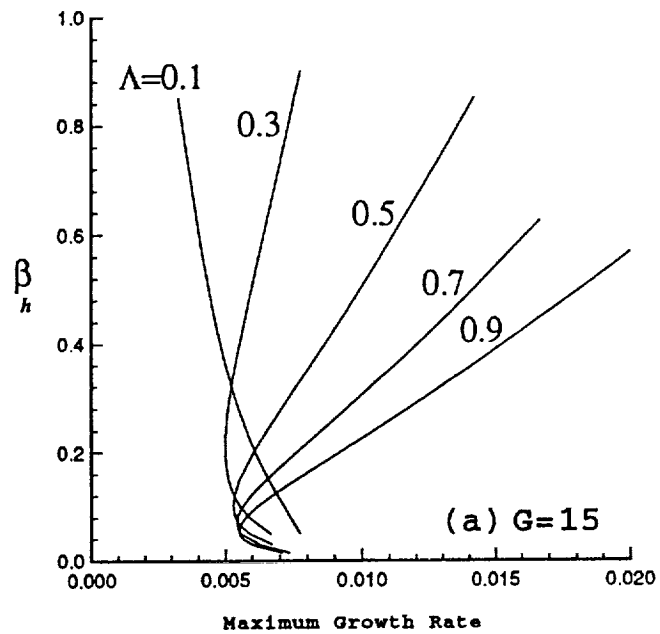


Figure 6. Effect of sweep angle and pressure gradient on maximum growth rate of stationary crossflow and Görtler disturbances of FSC boundary layer for two different Görtler numbers.

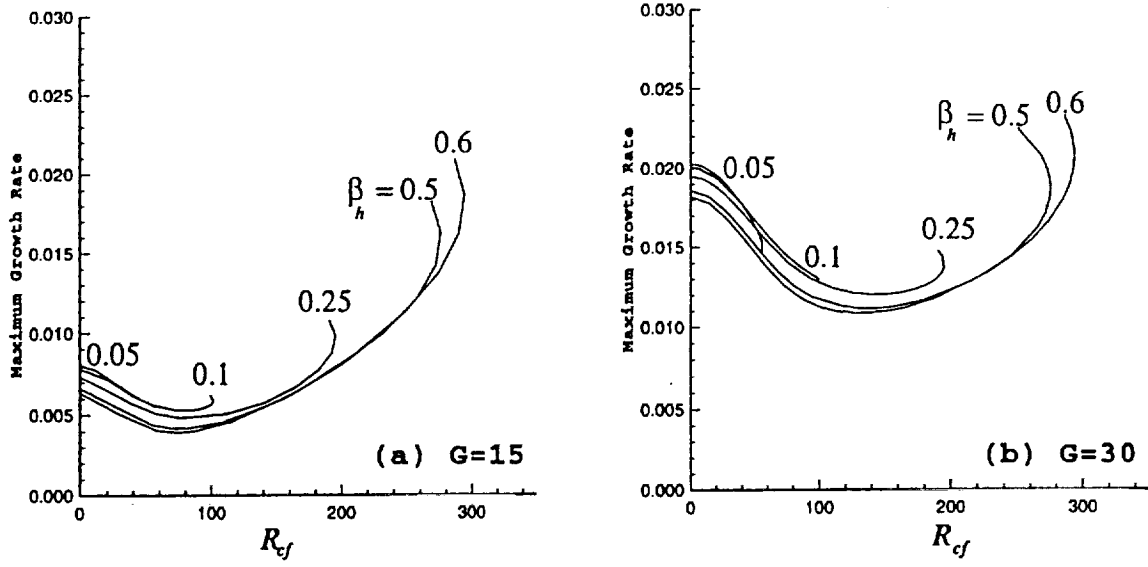


Figure 7. Variation of maximum growth rate with  $R_{cf}$  for fixed  $\beta_h$ .

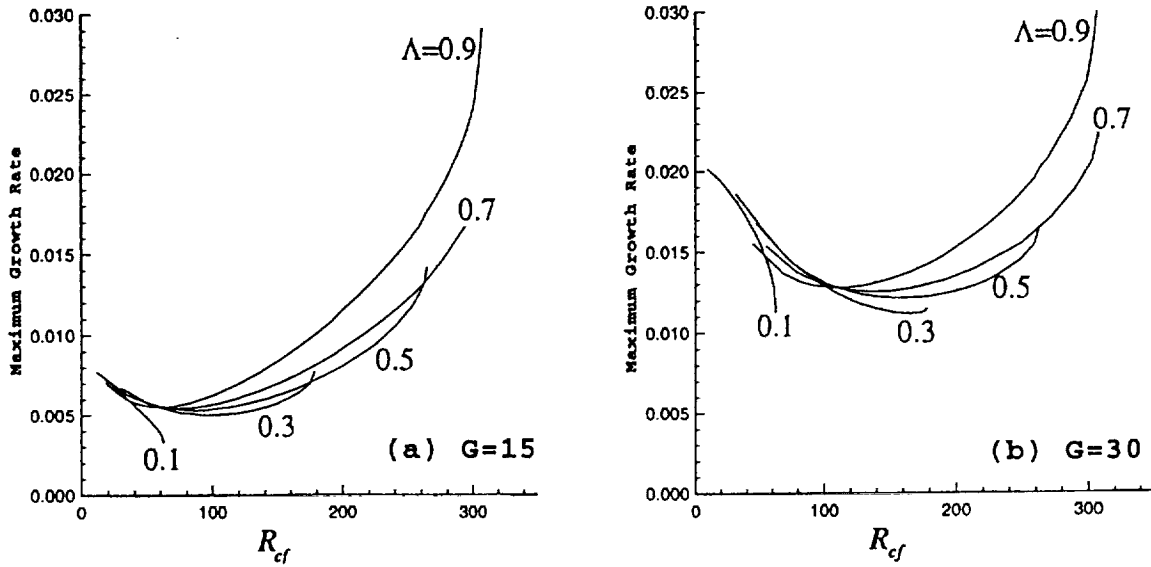


Figure 8. Variation of maximum growth rate with  $R_{cf}$  for fixed  $\Lambda$ .

REPORT DOCUMENTATION PAGE			Form Approved OMB No. 0704-0188	
Public reporting burden for this collection of information is estimated to average 1 hour per response, including the time for reviewing instructions, searching existing data sources, gathering and maintaining the data needed, and completing and reviewing the collection of information. Send comments regarding this burden estimate or any other aspect of this collection of information, including suggestions for reducing this burden, to Washington Headquarters Services, Directorate for Information Operations and Reports, 1215 Jefferson Davis Highway, Suite 1204, Arlington, VA 22202-4302, and to the Office of Management and Budget, Paperwork Reduction Project (0704-0188), Washington, DC 20503.				
1. AGENCY USE ONLY(Leave blank)	2. REPORT DATE November 1994	3. REPORT TYPE AND DATES COVERED Contractor Report		
4. TITLE AND SUBTITLE EFFECT OF CROSSFLOW ON GÖRTLER INSTABILITY IN IN-COMPRESSIBLE BOUNDARY LAYERS			5. FUNDING NUMBERS C NAS1-19480 WU 505-90-52-01	
6. AUTHOR(S) Y. H. Zurigat M. R. Malik				
7. PERFORMING ORGANIZATION NAME(S) AND ADDRESS(ES) Institute for Computer Applications in Science and Engineering Mail Stop 132C, NASA Langley Research Center Hampton, VA 23681-0001			8. PERFORMING ORGANIZATION REPORT NUMBER ICASE Report No. 94-94	
9. SPONSORING/MONITORING AGENCY NAME(S) AND ADDRESS(ES) National Aeronautics and Space Administration Langley Research Center Hampton, VA 23681-0001			10. SPONSORING/MONITORING AGENCY REPORT NUMBER NASA CR-195007 ICASE Report No. 94-94	
11. SUPPLEMENTARY NOTES Langley Technical Monitor: Michael F. Card Final Report To be submitted to Physics of Fluids				
12a. DISTRIBUTION/AVAILABILITY STATEMENT Unclassified-Unlimited  Subject Category 34			12b. DISTRIBUTION CODE	
13. ABSTRACT (Maximum 200 words) Linear stability theory is used to study the effect of crossflow on Gortler instability in incompressible boundary layers. The results cover a wide range of sweep angle, pressure gradient, and wall curvature parameters. It is shown that the crossflow stabilizes Gortler disturbances by reducing the maximum growth rate and shrinking the unstable band of spanwise wave numbers. On the other hand, the effect of concave wall curvature on crossflow instability is destabilizing. Calculations show that the changeover from Gortler to crossflow instabilities is a function of Gortler number, pressure gradient and sweep angle. The results demonstrate that Gortler instability may still be relevant in the transition process on swept wings even at large angles of sweep if the pressure gradient is sufficiently small. The influence of pressure gradient and sweep can be combined by defining a crossflow Reynolds number. Thus, the changeover from Gortler to crossflow instability takes place at some critical crossflow Reynolds number whose value increases with Gortler number.				
14. SUBJECT TERMS stability transition; Gortler; crossflow; three-dimensional boundary layers			15. NUMBER OF PAGES 19	
			16. PRICE CODE A03	
17. SECURITY CLASSIFICATION OF REPORT Unclassified	18. SECURITY CLASSIFICATION OF THIS PAGE Unclassified	19. SECURITY CLASSIFICATION OF ABSTRACT	20. LIMITATION OF ABSTRACT	